Journal of Statistical Mechanics: Theory and Experiment
An IOP and SISSA journal

PAPER: Classical statistical mechanics, equilibrium and non-equilibrium

Sorption–desorption, surface diffusion, and memory effects in a 3D system

P M Ndiaye[1], F W Tavares[1], E K Lenzi[2,*], L R Evangelista[3], H V Ribeiro[3], D Marin[2], L M S Guilherme[2] and R S Zola[3,4]

[1] Departamento de Engenharia Química, Escola de Química, Universidade Federal do Rio de Janeiro - Rio de Janeiro, RJ 21941-909, Brazil
[2] Departamento de Física, Universidade Estadual de Ponta Grossa - Ponta Grossa, PR 84030-900, Brazil
[3] Departamento de Física, Universidade Estadual de Maringá - Maringá, PR 87020-900, Brazil
[4] Department of Physics, Universidade Tecnológica Federal do Paraná - Apucarana, PR 86812-460, Brazil
E-mail: eklenzi@uepg.br

Received 23 May 2021
Accepted for publication 24 September 2021
Published 3 November 2021

Online at stacks.iop.org/JSTAT/2021/113202
https://doi.org/10.1088/1742-5468/ac2a9d

Abstract. Bio and nature behavior-inspired modelling of diffusion and trapping of particles, key phenomena for life occurrence, must consider a myriad of ingredients, such as geometry, dimensionality, and scaled diffusion processes occurring across the bulk and surfaces. To attempt to approach this goal, we investigate the diffusion process in a system limited by a surface connected to the bulk through an especially designed boundary condition, connected to some systems of interest, such as in living cells and biomaterials. The surface may sorb/desorb particles from the bulk and shows that the sorbed particles may diffuse within its structure, characterizing a lateral diffusion, before being desorbed back to the bulk. For this system, we find a wide variety of behaviors by analyzing solutions obtained in terms of the Green function approach. The analytical calculation is checked against computer simulations, demonstrating a good agreement between analytical calculation and stochastic computer simulation.

Keywords: Brownian motion, diffusion, stochastic particle dynamics, surface diffusion

*Author to whom any correspondence should be addressed.

1742-5468/21/113202+17$33.00

Contents

1. Introduction

Understanding the behavior of complex systems within different areas of science is challenging due to a wide variety of phenomena, particularly distinct bulk, surface, and interface effects that simultaneously define how the system behaves, self-arranges, and how it reacts to external stimuli. Diffusion and adsorption phenomena are definitely among such effects, often seen as essential in many scenarios for creating or facilitating other processes, like the ones necessary to sustain the biochemical reactions in living systems [1, 2]. They are also crucial factors in other contexts, including the electrical response of weak electrolytes [3] and liquid crystals [4, 5], in cancer invasion [6], population dynamics [7, 8], and several others [9–14], including neuronal growth on surfaces with controlled geometries [15]. When modeling diffusion and adsorption processes, it is widespread to assume that the system may be viewed as one-dimensional (1D) diffusion, and that once the surface traps the particles, it does not move within the surface [16–18]. Although 1D diffusion represents a good approximation in several systems, especially those with an elongated dimension (such as diffusion in pipes for example), most systems are essentially three-dimensional. In some cases, the 1D approximation may not be valid, as seems to be the case for protein targeting DNA molecules [19]. Adsorption phenomena are also frequently treated as if diffusion is not allowed to happen on the surface. However, the experimental results suggest that particles are diffusive within the surface, jumping from one adsorption site to another [20, 21]. Indeed, surface diffusion plays a major role in several systems [21], such as charge adsorption in supercapacitors [22], in the transport of adsorbed gas through shale [23, 24], in thin films [25], in surface-based biosensors [26] and many others. It is especially important for biological systems. For example, it was recently shown that long-term hippocampal potentiation and contextual learning require surface diffusion of postsynaptic AMPA receptors [27]. Antibody distribution in rats' brains has recently been shown to occur by diffusion at the brain's surface [28]. Perhaps the most striking example correlated with 3D diffusion followed by particle trapping and surface diffusion occurs in living cells, where different elements (nutrients or waste elements, for example) are diffusive until they reach the

J. Stat. Mech. (2021) 113202

cell membrane. In this scenario, several different phenomena may occur; among them, diffusion through and within the cell membrane, as is the case of small molecules diffusing through lipid bilayers and lateral diffusion of lipids within the bilayer [29–31]. Besides diffusion, another remarkable surface effect is related to a reaction at the surface; a phenomenon that is related to several technologies, including catalysts for producing fuel [32], in biochemical sensors [33], solar energy devices [34], and many others [35].

Inspired by the experimental systems described before and noticing a lack of theoretical models to account for such systems, we analyze a 3D diffusive system limited by a surface capable of adsorbing particles and, once adsorbed, allowing diffusion within the surface to occur. Furthermore, the model also accounts for reaction processes on the surface. The processes related to the surface (sorption–desorption) presence are governed by a kinetic equation that extends the usual one by incorporating memory effects and standard diffusion equation in the bulk. The equation's solution is obtained analytically by using the Green function approach and numerically by considering different situations to evaluate the diffusion effects on the surface processes. We find a wealthy class of diffusing regimes related to anomalous diffusion with the solutions obtained here, as is often reported for systems connected to the one reported here, especially in bio-systems.

2. The problem: diffusion and kinetics

Let us start our discussion about the diffusion and sorption–desorption processes by defining the region where the system diffuses and the properties of the surface are in contact with this region (bulk). We consider a three-dimensional system defined by the Cartesian coordinates, i.e. $\mathbf{r} = (x, y, z)$, with a surface located at $z = 0$. Thus, the system is set in a semi-infinite region as illustrated in figure 1, where diffusion in the bulk is represented in green, whereas three adsorbed particles and their respective diffusions on the substrate are represented in black, blue, and red. The surface may adsorb particles and desorb (or release) particles to the bulk, with a characteristic rate (described below). The particles adsorbed by the surface may diffuse on the surface before desorption to the bulk, or, if not allowed to diffuse within the surface (surface diffusion coefficient equal to zero), stay in a resting position before desorption. This shift in the region in which the particles are diffusing (from where the particles left the bulk to where they are desorbed to it) causes a change in the mechanism of the diffusion of the system. We observed two different types of diffusion in the system: one related to the free particles in the bulk and another one related to the particles on the surface.

To describe the entire system, two diffusion equations associated with the bulk and the surface are necessary in the bulk, the diffusion is governed by the following equation:

$$\frac{\partial}{\partial t}\rho(\mathbf{r}, t) = \mathcal{K}_{b,\parallel}\nabla^2_{\parallel}\rho(\mathbf{r}, t) + \mathcal{K}_{b,\perp}\nabla^2_{\perp}\rho(\mathbf{r}, t), \tag{1}$$

J. Stat. Mech. (2021) 113202

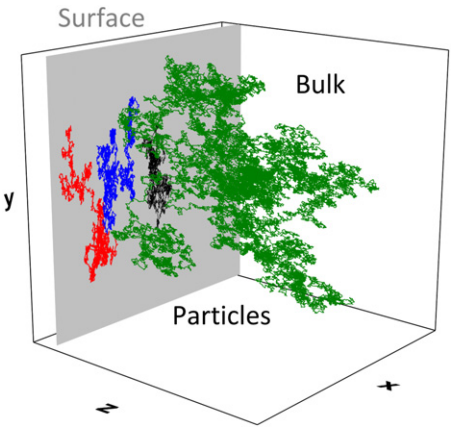

Figure 1. From right to left: an illustrative particle diffusing in bulk is adsorbed by the surface and diffuses among the surface. From left to right: the particle once adsorbed by the surface disengages from it and still diffuses in the bulk.

where $\nabla_{\perp}^2 = \partial_z^2$ and $\nabla_{\parallel}^2 = \partial_x^2 + \partial_y^2$, where $\mathbf{r}_{\parallel} = x\hat{\mathbf{x}} + y\hat{\mathbf{y}}$ and $\mathbf{r}_{\perp} = z\hat{\mathbf{z}}$. $\mathcal{K}_{b,\parallel}$ and $\mathcal{K}_{b,\perp}$ are the diffusion coefficients on the parallel and perpendicular directions, and $\rho(\mathbf{r}, t)$ represents the distribution of particles in the bulk. Note that diffusion coefficients $\mathcal{K}_{b,\parallel}$ and $\mathcal{K}_{b,\perp}$ are connected to the diffusion on the plane (x, y) and in the perpendicular direction, z, respectively. This choice enables us to consider anisotropic situations and, in particular, the scenarios in which the diffusion coefficient on the surface is the same as the bulk on the plane (x, y). For the isotropic situations, we have that $\mathcal{K}_{b,\parallel} = \mathcal{K}_{b,\perp}$ in the bulk.

For the processes occurring on the surface, the following equation is used [36]:

$$\frac{\partial}{\partial t}\mathcal{C}(\mathbf{r}_{\parallel}, t) = \mathcal{K}_s \nabla_{\parallel}^2 \mathcal{C}(\mathbf{r}_{\parallel}, t) + \int_0^t \mathrm{d}t' k_s(t - t')\rho(\mathbf{r}, t')|_{z=0} - k_d \mathcal{C}(\mathbf{r}_{\parallel}, t), \tag{2}$$

where $\mathcal{K}_s$ is the diffusion coefficient for the particles' concentration (or distribution) on the surface, $\mathcal{C}(\mathbf{r}_{\parallel}, t)$ represents the particles on the surface, k_d is the rate of desorption, and $k_s(t)$ is a kernel defining the nature of the adsorption process, that is, how important the preceding state of the particle in the bulk is for the adsorption process (see figure 1). It turns out that adsorption–desorption phenomena may follow non-exponential decay behavior, depending on the nature of the surface-particle's interaction. For example, for pure physisorption processes, a particle with specific energy may fall into an adsorption well and lose some of its energy, but get desorbed back to the bulk after a while. If such a particle is adsorbed again, the amount of energy lost in the previous process is relevant to determine how the following process takes place. Thus, the next state depends on the previous one, which characterizes a non-Markovian process, that is, a memory effect [16]. In particular, if $k_s(t) = \kappa\delta(t)$, the kernel is a localized function of time, meaning the preceding state does not matter, so k_s is constant, representing a constant rate of adsorption. If, for example, $k_s(t) = \kappa\left(e^{-t/\tau_a}/\tau_a\right)$, the kernel is a long-range function of time, meaning there is a memory effect in the adsorption process, with memory time τ_a [18]. Thus, in the kernels above, the parameter κ is the rate of adsorption, while the parameter τ_a represents memory time. It is also interesting to note that for $\tau_a \to 0$,

J. Stat. Mech. (2021) 113202

the previous process is recovered. In a few words, equation (2) is a balance equation that states that the time variation of particles in the surface is equal to the gradient of particles within the surface; that is, it depends on the diffusion on the surface, plus the amount of particles right in front of the surface, available to be adsorbed, minus the amount desorbed back to the bulk. It is a linear version of the Langmuir kinetic equation [37] with memory effects and surface diffusion. This equation is also coupled with equation (1) by the presence of the term $\int_0^t \mathrm{d}t'\, k_s(t-t')\rho(\mathbf{r},t')|_{z=0}$.

In order to represent an adsorption and desorption process, governed by the rates $k_s(t)$ and $k_d(t)$, we connect them, i.e. equations (1) and (2), in $z=0$ by the boundary condition:

$$\mathcal{K}_{b,\perp}\left(\mathbf{n}\cdot\nabla_\perp\rho\right)|_{z=0} = \frac{\mathrm{d}}{\mathrm{d}t}\mathcal{C}(\mathbf{r}_\parallel,t) + \int_0^t \mathrm{d}t'\, k_r(t-t')\rho(\mathbf{r},t)|_{z=0}. \tag{3}$$

The first term on the right-hand side of equation (3) is related to the adsorption–desorption processes between the surface and bulk, and the second term represents a reaction (see, for example, [38, 39]) process that implies a removal of the particles from the bulk to the surface. Note that the last term depends on the choice of $k_r(t)$, which determines the reaction processes connected to the removal (or immobilization) of the particles from the bulk by the surface. Therefore, adsorbed particles are diffusive on the surface and are desorbed with the rate k_d or promote a reaction process on the surface with the rate k_r. Additional boundary conditions to analyze the problem defined above are $\partial_z\rho(\mathbf{r},t)|_{z\to\infty}=0$, $\partial_x\rho(\mathbf{r},t)|_{x\to\pm\infty}=0, \partial_y\rho(\mathbf{r},t)|_{y\to\pm\infty}=0$ $\partial_x\mathcal{C}(\mathbf{r}_\parallel,t)\big|_{x\to\pm\infty}=0$, and $\partial_y\mathcal{C}(\mathbf{r}_\parallel,t)\big|_{y\to\pm\infty}=0$. We consider the system initially defined by the conditions, $\rho(\mathbf{r},0)=\varphi(\mathbf{r})$ (so any initial configuration is allowed in the bulk) and, for simplicity, $\mathcal{C}(\mathbf{r}_\parallel,0)=0$, which implies that initially all of the particles are in the bulk.

By using the boundary conditions, it is possible to analyze the modifications produced on the system by the processes taking place on the surface. In particular, by incorporating the previous equations on the diffusion equation, we have

$$\frac{\mathrm{d}}{\mathrm{d}t}\left(\int \mathrm{d}\mathbf{r}_\perp \int \mathrm{d}\mathbf{r}_\parallel \rho(\mathbf{r},t) + \int \mathcal{C}(\mathbf{r}_\parallel,t)\mathrm{d}\mathbf{r}_\parallel\right) = -\int_0^t k_r(t-t')\int \rho(\mathbf{r},t')\Big|_{z=0}\mathrm{d}\mathbf{r}_\parallel \mathrm{d}t', \tag{4}$$

where the term on the right side, with $k_r(t)$, implies a reaction process where the particles are removed (or immobilized) from the bulk by the surface, as discussed before. For the particular case where $k_r(t)=0$, it is possible to show that

$$\int \mathrm{d}\mathbf{r}_\perp \int \mathrm{d}\mathbf{r}_\parallel\, \rho(\mathbf{r},t) + \int \mathrm{d}\mathbf{r}_\parallel\, \mathcal{C}(\mathbf{r}_\parallel,t) = \text{constant}, \tag{5}$$

which is a direct consequence of the conservation of the total number of particles present in the system.

J. Stat. Mech. (2021) 113202

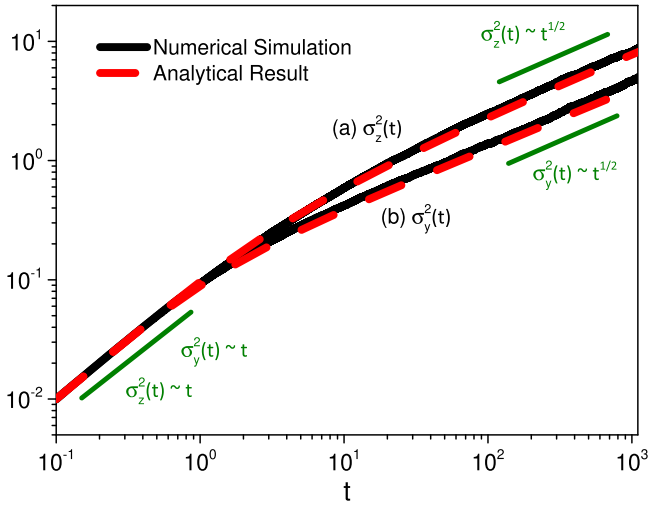

Figure 2. The MSD of the distribution for the z- and y-directions in the bulk, when an absorbent surface is considered. The numerical simulation considers the Langevin equation with white noise and an exponential distribution for the desorption process of the particles from the surface to the bulk; for this case, the Poisson distribution was used with the mean one. We used $\mathcal{K}_S = \mathcal{K}_\parallel = \mathcal{K}_\perp = 5 \times 10^{-2}$ and $z' = 1/2$, in arbitrary units.

3. Behavior of $\rho(\mathbf{r}, t)$ and $\mathcal{C}(\mathbf{r}_\parallel, t)$

Let us focus our attention on the spatial and time behavior of the particles on the surface and in the bulk. We start by obtaining the solution for this problem, i.e. $\rho(\mathbf{r}, t)$ and $\mathcal{C}(\mathbf{r}_\parallel, t)$, which implies solving the previous coupled set of equations. In this sense, we use integral transforms (Fourier and Laplace) and the Green function approach [40]. Thus, in the Laplace ($t \to s$) and Fourier ($\mathbf{r}_\parallel \to \mathbf{k}_\parallel$) spaces, the solution of equations (1) and (2) are given by

$$\rho(\mathbf{k}_\parallel, z, s) = -\int_0^\infty \mathrm{d}z' \varphi(\mathbf{k}_\parallel, z') \mathcal{G}(\mathbf{k}_\parallel, z, z', s) + s\mathcal{C}(\mathbf{k}_\parallel, s) \mathcal{G}(\mathbf{k}_\parallel, 0, z', s), \tag{6}$$

and

$$\mathcal{C}(\mathbf{k}_\parallel, s) = \frac{k_s(s)}{s + \mathcal{K}_s k_\parallel^2 + k_d} \rho(\mathbf{k}_\parallel, 0, s), \tag{7}$$

with the Green function given by

$$\mathcal{G}(\mathbf{k}_\parallel, z, z', s) = -\frac{e^{-\sqrt{s + \mathcal{K}_{b,\parallel} k_\parallel^2} \frac{|z - z'|}{\sqrt{\mathcal{K}_{b,\perp}}}}}{2\sqrt{\left(s + \mathcal{K}_{b,\parallel} \mathbf{k}_\parallel^2\right) \mathcal{K}_{b,\perp}}}$$

J. Stat. Mech. (2021) 113202

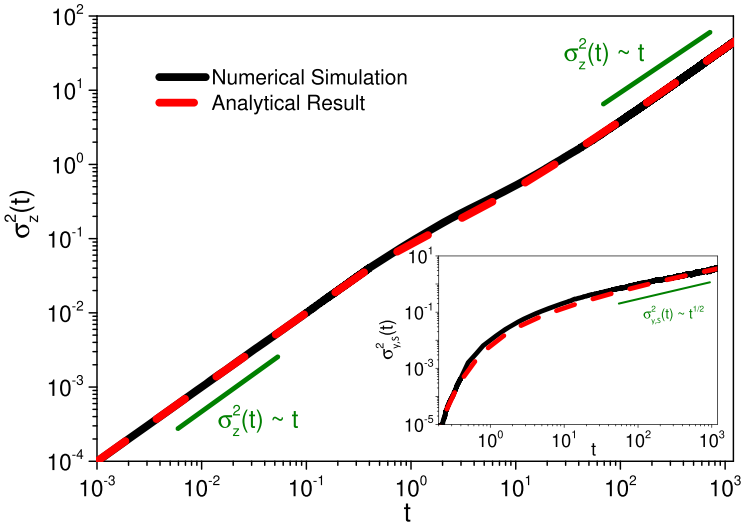

Figure 3. The MSD of the distribution for the z-direction and for the y-direction on the surface. The particles diffuse in the bulk and may be adsorbed and desorbed on the surface. It may also diffuse on the surface before being desorbed to the bulk. The numerical simulation considers the Langevin equation with white noise and an exponential distribution for the desorption process of the particles from the surface to the bulk. For this case, it was used the Poisson distribution with a mean one. We used $\mathcal{K}_S = \mathcal{K}_\parallel = \mathcal{K}_\perp = 5 \times 10^{-2}$, $k_d = 10$, $\kappa = 5$, and $z' = 1/2$, in arbitrary units.

$$-\frac{1}{2\sqrt{\left(s+\mathcal{K}_{b,\parallel}k_\parallel^2\right)\mathcal{K}_{b,\perp}}}\frac{\sqrt{\left(s+\mathcal{K}_{b,\parallel}k_\parallel^2\right)\mathcal{K}_{b,\perp}}-k_r(s)}{\sqrt{\left(s+\mathcal{K}_{b,\parallel}k_\parallel^2\right)\mathcal{K}_{b,\perp}}+k_r(s)}e^{-\sqrt{s+\mathcal{K}_{b,\parallel}k_\parallel^2}\frac{|z+z'|}{\sqrt{\mathcal{K}_{b,\perp}}}}, \tag{8}$$

which was obtained from the following equation

$$\mathcal{K}_{b,\perp}\frac{\partial^2}{\partial z^2}\mathcal{G}(\mathbf{k}_\parallel,z,z',s)-\left(s+\mathcal{K}_{b,\parallel}\mathbf{k}_\parallel^2\right)\mathcal{G}(\mathbf{k}_\parallel,z,z',s)=\delta(z-z'), \tag{9}$$

subjected to the boundary conditions

$$\mathcal{K}_{b,\perp}\frac{\partial}{\partial z}\mathcal{G}(\mathbf{k}_\parallel,z,z',s)\Big|_{z=0}-k_r(s)\mathcal{G}(\mathbf{k}_\parallel,0,z',s)=0, \tag{10}$$

and $\mathcal{G}(\mathbf{k}_\parallel,\infty,z',s)=0$. For the particular case $k_r(s)=k_r=\text{const}$ (or $k_r(t)=k_r\delta(t)$), the previous Green function, after performing the inverse of Laplace and Fourier transforms, yields

$$\begin{aligned}\mathcal{G}(\mathbf{r}_\parallel,z,z',t)=&-\mathcal{G}_{\mathcal{K}_{b,\parallel}}(\mathbf{r}_\parallel,t)\left[\mathcal{G}_{\mathcal{K}_{b,\perp}}(z-z',t)-\mathcal{G}_{\mathcal{K}_{b,\perp}}(z+z',t)\right]\\&-\mathcal{G}_{\mathcal{K}_{b,\parallel}}(\mathbf{r}_\parallel,t)\int_0^t \mathrm{d}t'\Phi(t-t')\mathcal{G}^{(1)}_{\mathcal{K}_{b,\perp}}(z+z',t)\end{aligned} \tag{11}$$

J. Stat. Mech. (2021) 113202

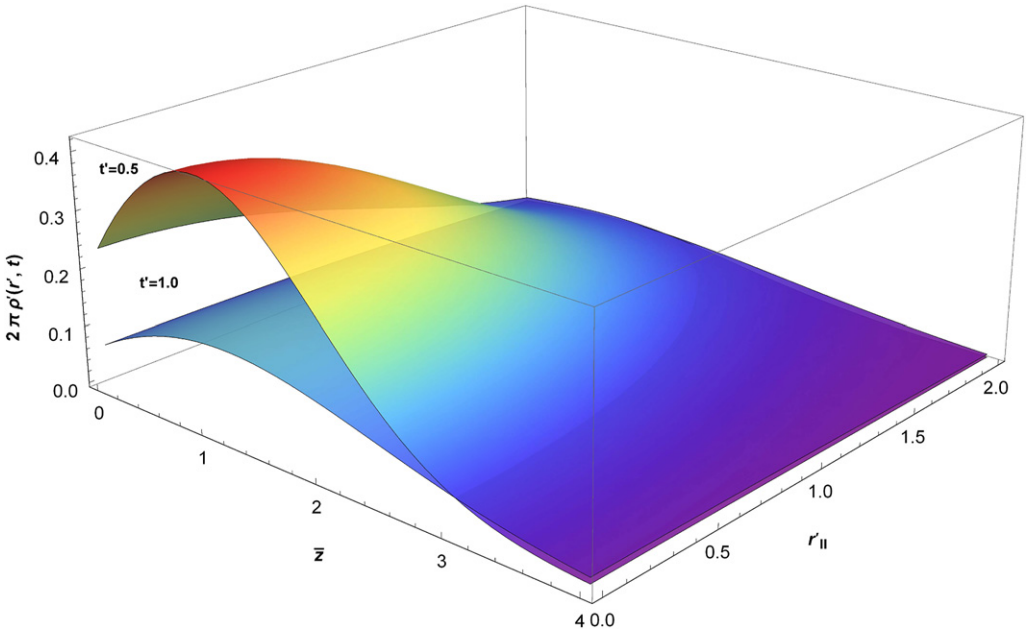

Figure 4. Behavior of $2\pi\rho'(\mathbf{r}',t)$ versus $r'_{\parallel}$ and $\bar{z}$ for $t'=0.5$ and $t'=1$, where $\rho'(\mathbf{r},t)=z'^{3}\rho(\mathbf{r},t)$, $r'_{\parallel}=r_{\parallel}/z'$, and $\bar{z}=z/z'$. We consider, for simplicity, $\mathcal{K}_s/\mathcal{K}_{b,\perp}=1/2$, $k'_d=z'^{2}k_d/\mathcal{K}_{b,\perp}=0.1$, $z'\kappa/\mathcal{K}_{b,\perp}=1$, $k_r=0$, $t'=z'^{2}t/\mathcal{K}_{b,\perp}$, and $\mathcal{K}_{b,\parallel}/\mathcal{K}_{b,\perp}=1$.

with

$$\mathcal{G}_{\mathcal{K}_{b,\parallel}}(\mathbf{r}_{\parallel},t)=\frac{e^{-\frac{|\mathbf{r}_{\parallel}|^2}{4\mathcal{K}_{b,\parallel}t}}}{4\pi\mathcal{K}_{b,\parallel}t},\ \mathcal{G}_{\mathcal{K}_{b,\perp}}(z,t)=\frac{e^{-\frac{z^2}{4\mathcal{K}_{b,\perp}t}}}{\sqrt{4\pi\mathcal{K}_{b,\perp}t}},\ \mathcal{G}^{(1)}_{\mathcal{K}_{b,\perp}}(z,t)=\frac{|z|e^{-\frac{z^2}{4\mathcal{K}_{b,\perp}t}}}{2t\sqrt{\pi\mathcal{K}_{b,\perp}t}},\quad(12)$$

and $\Phi(t)=1/\sqrt{\pi\mathcal{K}_{b,\perp}t}-(k_r/\mathcal{K}_{b,\perp})\,e^{k_r^2t/\mathcal{K}_{b,\perp}}\,\mathrm{erfc}\left(k_r\sqrt{t/\mathcal{K}_{b,\perp}}\right)$, where $\mathrm{erfc}(x)$ is the complementary error function. By using these results, it is possible to obtain the behavior of the particles in the bulk and the surface. In particular, before the inversion procedures, we have

$$\mathcal{C}(\mathbf{k}_{\parallel},s)=-\frac{k_s(s)\left(\sqrt{\left(s+\mathcal{K}_{b,\parallel}k_{\parallel}^2\right)\mathcal{K}_{b,\perp}}+k_r(s)\right)}{\left(s+\mathcal{K}_sk_{\parallel}^2+k_d\right)\left(\sqrt{\left(s+\mathcal{K}_{b,\parallel}k_{\parallel}^2\right)\mathcal{K}_{b,\perp}}+k_r(s)\right)+sk_s(s)}$$
$$\times\int_0^{\infty}\mathrm{d}z'\,\varphi(\mathbf{k}_{\parallel},z')\mathcal{G}(\mathbf{k}_{\parallel},0,z',s)\quad(13)$$

J. Stat. Mech. (2021) 113202

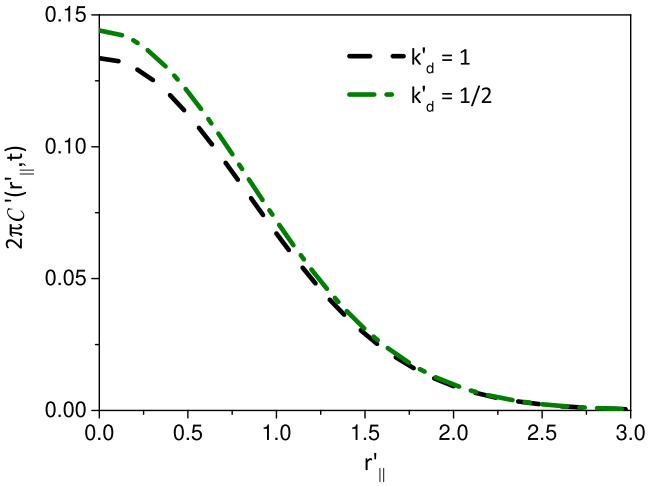

Figure 5. Trend of $\mathcal{C}'(\mathbf{r}_\parallel, t)$ versus $r'_\parallel$, for $k_r = 0$ and $t' = 1/2$, where $\mathcal{C}(\mathbf{r}_\parallel, t) = z'^2\mathcal{C}'(\mathbf{r}_\parallel, t)$, $t' = z'^2 t/\mathcal{K}_{b,\perp}$, and $r'_\parallel = r_\parallel/z'$. The curves were drawn for $\mathcal{K}_s/\mathcal{K}_{b,\perp} = 1/2$, $k'_d = z'^2 k_d/\mathcal{K}_{b,\perp}$, $z'\kappa/\mathcal{K}_{b,\perp} = 1$, and $\mathcal{K}_{b,\parallel}/\mathcal{K}_{b,\perp} = 1$.

and

$$\rho(\mathbf{k}_\parallel, 0, s) = -\frac{\left(s + \mathcal{K}_s k_\parallel^2 + k_d\right)\left(\sqrt{\left(s + \mathcal{K}_{b,\parallel} k_\parallel^2\right)\mathcal{K}_{b,\perp}} + k_r(s)\right)}{\left(s + \mathcal{K}_s k_\parallel^2 + k_d\right)\left(\sqrt{\left(s + \mathcal{K}_{b,\parallel} k_\parallel^2\right)\mathcal{K}_{b,\perp}} + k_r(s)\right) + s k_s(s)} \times \int_0^\infty \mathrm{d}z'\, \varphi(\mathbf{k}_\parallel, z')\mathcal{G}(\mathbf{k}_\parallel, 0, z', s). \tag{14}$$

The particular case $k_r(s) = k_r = \text{const}$ (or $k_r(t) = k_r\delta(t)$), after performing the inverse Laplace and Fourier transforms, yields

$$\mathcal{C}(\mathbf{r}_\parallel, t) = \Omega(\mathbf{r}_\parallel, t) + \sum_{n=1}^{\infty}(-1)^n \int_0^t \mathrm{d}t_n \int_{\mathcal{S}} \mathrm{d}\mathcal{A}_n \mathfrak{C}(\mathbf{r}_\parallel - \mathbf{r}_{\parallel,n}, t - t_n)\ldots \times \int_0^{t_2} \mathrm{d}t_1 \int_{\mathcal{S}} \mathrm{d}\mathcal{A}_1 \mathfrak{C}(\mathbf{r}_\parallel - \mathbf{r}_{\parallel,1}, t_2 - t_1)\Omega(\mathbf{r}_{\parallel,1}, t_1) \tag{15}$$

and

$$\rho(\mathbf{r}_\parallel, 0, t) = \mathcal{P}_0(\mathbf{r}_\parallel, t) + \sum_{n=1}^{\infty}(-1)^n \int_0^t \mathrm{d}t_n \int_{\mathcal{S}} \mathrm{d}\mathcal{A}_n \mathfrak{C}(\mathbf{r}_\parallel - \mathbf{r}_{\parallel,n}, t - t_n)\ldots \times \int_0^{t_2} \mathrm{d}t_1 \int_{\mathcal{S}} \mathrm{d}\mathcal{A}_1 \mathfrak{C}(\mathbf{r}_\parallel - \mathbf{r}_{\parallel,1}, t_2 - t_1)\mathcal{P}_0(\mathbf{r}_{\parallel,1}, t_1), \tag{16}$$

with

$$\mathfrak{C}(\mathbf{r}_\parallel, t) = \int_0^t \mathrm{d}t' k_s(t - t')\Phi(t')\mathcal{G}_{\mathcal{K}_\mathcal{S}}(\mathbf{r}_\parallel, t') - \int_0^t \int_{\mathcal{S}} \mathrm{d}\mathcal{A}' \Upsilon(\mathbf{r}_\parallel - \mathbf{r}'_\parallel, t - t')\Phi(t')\mathcal{G}_\mathcal{S}(\mathbf{r}'_\parallel, t'), \tag{17}$$

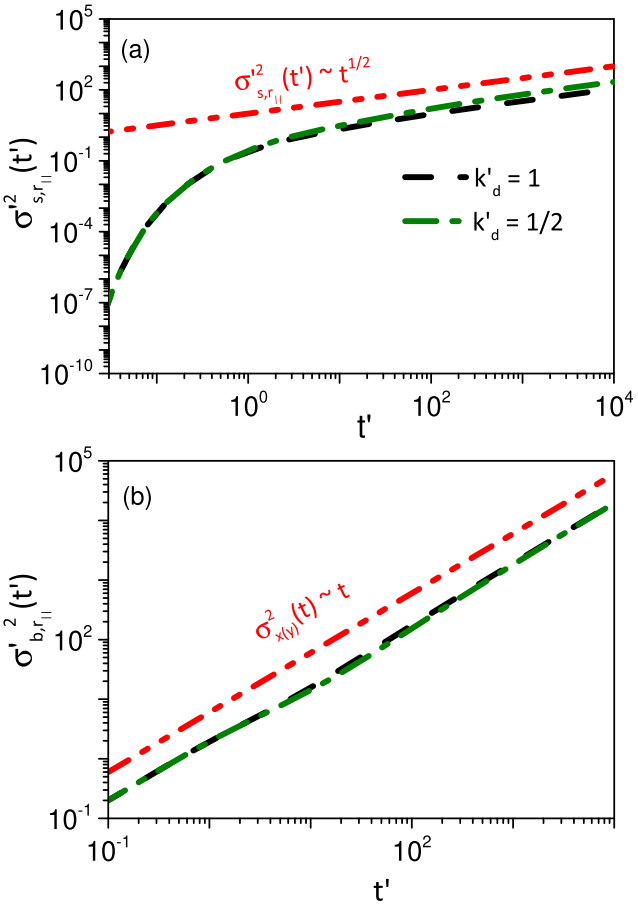

Figure 6. (a) $\sigma'^2_{s,r_\parallel}(t')$ versus t', where $\sigma^2_{s,r_\parallel}(t) = z'^2\sigma'^2_{s,r_\parallel}(t')$ and $t' = \mathcal{K}_{b,\perp}t/z'^2$. (b) $\sigma'^2_{b,r_\parallel}(t')$ versus t', where $\sigma^2_{b,r_\parallel}(t') = z'^2\sigma'^2_{b,r_\parallel}(t')$ and $t' = \mathcal{K}_{b,\perp}t/z'^2$. The curves were drawn for $\mathcal{K}_s/\mathcal{K}_{b,\parallel} = 1/2$, $k'_d = z'^2k_d/\mathcal{K}_{b,\perp}$, $k'_s = z'\kappa/\mathcal{K}_{b,\perp} = 1$, $k_r = 0$, and $\mathcal{K}_{b,\parallel}/\mathcal{K}_{b,\perp} = 1$.

where $\int_{\mathcal{S}}\mathrm{d}\mathcal{A}\ldots = \int_{-\infty}^{\infty}\mathrm{d}y\int_{-\infty}^{\infty}\mathrm{d}x\ldots$, $\Upsilon(\mathbf{r}_\parallel,t) = \int_0^t \mathrm{d}t' k_s(t-t')\partial_{t'}\left(e^{-k_dt'}\mathcal{G}_{\mathcal{K}_\mathcal{S}}(\mathbf{r}_\parallel,t')\right)$,

$$\Omega(\mathbf{r}_\parallel,t) = \int_0^t \mathrm{d}t' \int_{\mathcal{S}} \mathrm{d}\mathcal{A}' e^{-k_d(t-t')}\mathcal{G}_{\mathcal{K}_\mathcal{S}}(\mathbf{r}_\parallel - \mathbf{r}'_\parallel, t-t') \int_0^{t'} \mathrm{d}t'' k_s(t'-t'')\mathcal{P}_0(\mathbf{r}_\parallel,t'), \tag{18}$$

and

$$\mathcal{P}_0(\mathbf{r}_\parallel,t) = -\int_0^\infty \mathrm{d}z' \int_{\mathcal{S}} \mathrm{d}\mathcal{A}'\varphi(\mathbf{r}')\mathcal{G}(\mathbf{r}_\parallel - \mathbf{r}'_\parallel, 0, z', t), \tag{19}$$

J. Stat. Mech. (2021) 113202

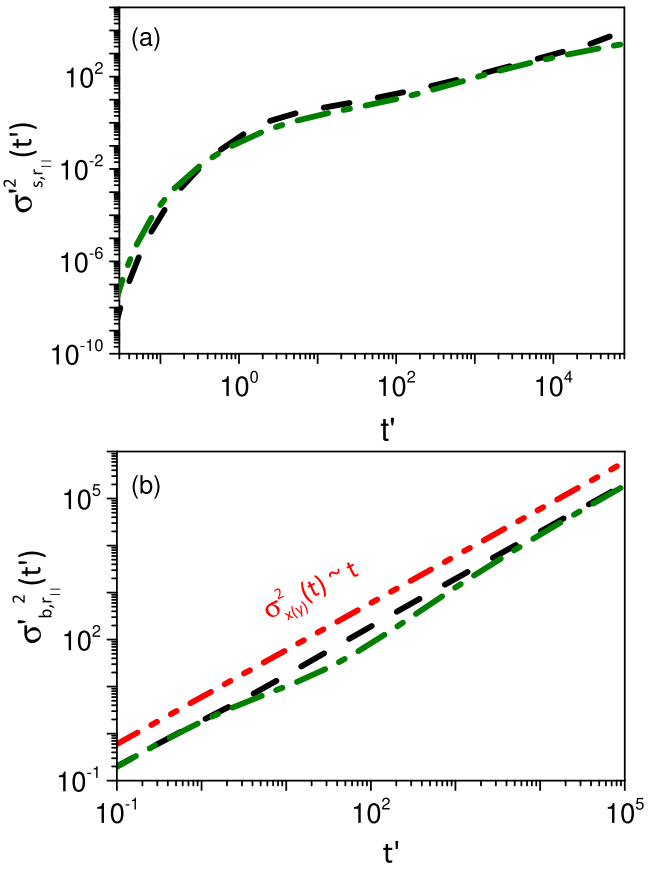

Figure 7. (a) $\sigma'^{2}_{s,r_{\parallel}}(t')$ versus t', where $\sigma^{2}_{s,r_{\parallel}}(t) = z'^{2}\sigma'^{2}_{s,r_{\parallel}}(t')$ and $t' = \mathcal{K}_{b,\perp}t/z'^{2}$. (b) $\sigma'^{2}_{b,r_{\parallel}}(t')$ versus t', where $\sigma^{2}_{b,r_{\parallel}}(t') = z'^{2}\sigma'^{2}_{b,r_{\perp}}(t')$ and $t' = \mathcal{K}_{b,\parallel}t/z'^{2}$. The black dashed line considers $k_s(t) = \kappa/\sqrt{\pi t}$ ($k_s(s) = \kappa/\sqrt{s}$ and green dashed-dotted line corresponds to the case $k_s(t) = \kappa/\sqrt{\pi t} - \kappa e^{t}\,\mathrm{erfc}\left(\sqrt{t}\right)$ ($k_s(s) = \kappa/(1+\sqrt{s})$). The curves were drawn for $\mathcal{K}_s/\mathcal{K}_{b,\parallel} = 1/2$, $k'_d = z'^{2}k_d/\mathcal{K}_{b,\parallel}$, $k'_s = z'\kappa/\mathcal{K}_{b,\perp} = 1$, $k_r = 0$, and $\mathcal{K}_{b,\parallel}/\mathcal{K}_{b,\perp} = 1$.

with $\mathcal{G}_{\mathcal{K}_{\mathcal{S}}}(\mathbf{r}_{\parallel}, t') = \mathcal{G}_{\mathcal{K}_{\parallel}}(\mathbf{r}_{\parallel}, t')$ for $\mathcal{K}_{\parallel} \to \mathcal{K}_{\mathcal{S}}$. By using the previous results, the particle distribution in the bulk is given by the following equation:

$$\rho(\mathbf{r}, t) = -\int_{\mathcal{S}} \mathrm{d}\mathcal{A}' \int_0^{\infty} \mathrm{d}z' \varphi(\mathbf{r}'_{\parallel}, z') \mathcal{G}(\mathbf{r}_{\parallel} - \mathbf{r}'_{\parallel}, z, z', t) + \int_{\mathcal{S}} \mathrm{d}\mathcal{A}' \int_0^{t} \mathrm{d}t' \mathcal{G}(\mathbf{r}_{\parallel} - \mathbf{r}'_{\parallel}, 0, z, t - t') \frac{\partial}{\partial t'} \mathcal{C}(\mathbf{r}'_{\parallel}, t'). \tag{20}$$

Before analyzing the analytical results obtained so far, let us consider a stochastic simulation to gain more insight related to the equations above for the probability distribution. In other words, in order to compare the analytical solutions coming from the diffusion equation and the kinetic equation, we performed numerical simulations by using a different method. To do this, the Langevin equation is simulated by considering particles in three dimensions with a surface that may absorb or adsorb/desorb particles with a

J. Stat. Mech. (2021) 113202

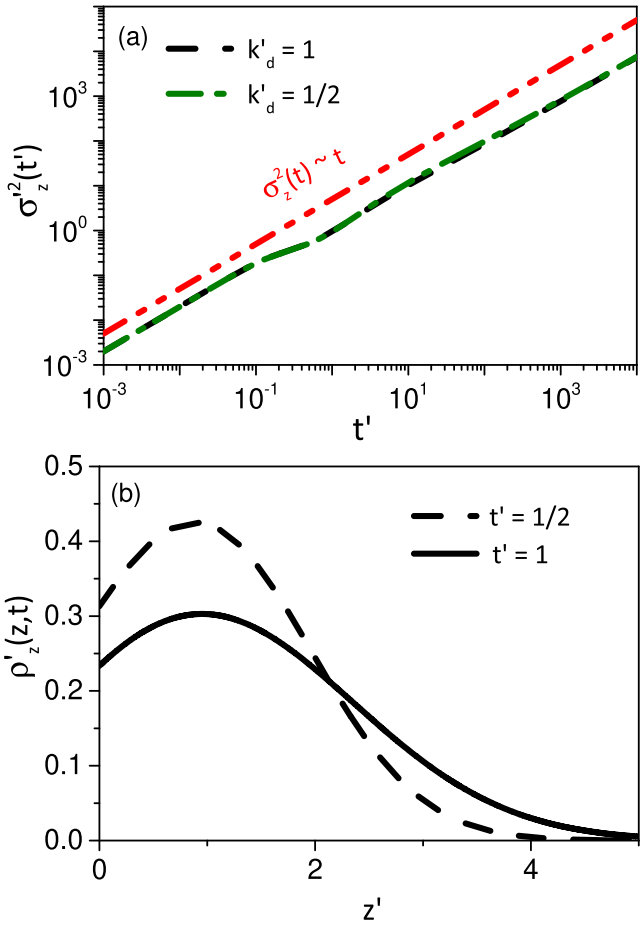

Figure 8. (a) $\sigma_z'^2(t')$ versus t', where $\sigma_z^2(t') = z'^2\sigma_z'(t)$ and $t' = \mathcal{K}_{b,\perp}t/z'^2$. (b) $\rho_z'(z,t)$ versus $\bar{z}$, where $\rho_z'(z,t) = z'\rho_z(z,t)$, $\bar{z} = z/z'$, and $k_d' = 0.1$. We used $z'^2k_d/\mathcal{K}_{b,\perp} = 1$, $z'\kappa/\mathcal{K}_{b,\perp} = 1/2$, and $\mathcal{K}_{b,\parallel}/\mathcal{K}_{b,\perp} = 1$.

characteristic kinetic process. We consider for the numerical simulation the following stochastic equations:

$$\dot{x} = \sqrt{2\mathcal{D}}\xi_x(t), \quad \dot{y} = \sqrt{2\mathcal{D}}\xi_y(t), \quad \text{and} \quad \dot{z} = \sqrt{2\mathcal{D}}\xi_z(t), \tag{21}$$

where $\xi_i(t)$ (with $i = x, y, z$) represents the noise in each direction with $\langle\xi_i(t)\rangle = 0$, $\langle\xi_i(t)\xi_j(t)\rangle = 0$, and $\langle\xi_i(t)\xi_i(t')\rangle \propto \delta(t-t')$. Equations (21) were analyzed by using the Euler method to perform the numerical calculations [41] under different scenarios. The first case analyzed concerns an absorbent surface, which is characterized by the boundary conditions $\rho(\mathbf{r},t)|_{z=0} = 0$, $\rho(\mathbf{r},t)|_{z=\infty} = 0$, $\partial_x\rho(\mathbf{r},t)|_{x\to\pm\infty} = 0$, and $\partial_y\rho(\mathbf{r},t)|_{y\to\pm\infty} = 0$. Next, an adsorption–desorption was simulated by considering that particles are subjected to an exponential distribution of time for permanence on the surface, but the particles do not diffuse on the surface. We obtain the mean square displacement (MSD) from these numerical simulations, and, consequently, the diffusive behavior (time dependence) of the same system presented before for the analytical model. The MSD evaluation from the numerical point of view is performed by considering the Langevin equations for the

J. Stat. Mech. (2021) 113202

particles on the surface and in the bulk to analyze each case. We also consider distributions to simulate the adsorption–desorption process. Thus, the MSD is evaluated for each case, surface and bulk, by considering a Langevin equation for each particle, with numerous replicas to evaluate the averages. In particular, we have considered 5×10^4 replicas to perform the calculation of the MSD. The evaluation is carried out by tracking each particle motion and computing the MSD when it takes place in the bulk and on the surface. We have considered that the particles were initially in a position to start the motion governed by the Langevin equation. After some time, the particles reach the surface and are adsorbed. In particular, the criterion used to define that the particle reached the surface is a simple boundary crossing, i.e. $x \leqslant 0$ implies that the particle reaches the surface. The permanence of the surface is defined by the distribution of times, while, on the surface, the particle also diffuses, governed by the Langevin equation. The displacements in the bulk and on the surface are used to obtain the MSD in each case.

For the first scenario, i.e. absorbing surfaces without surface diffusion, the mean square displacements in the z- and y-directions are shown in figure 2. In this figure, we also show the result obtained from equation (20) for absorbing boundary conditions, which for the one dimensional case, with the diffusion in the z-direction, implies that

$$\rho(\mathbf{r},t) = \int_{\mathcal{S}} \mathrm{d}\mathcal{A}' \int_0^\infty \mathrm{d}z' \varphi(z') \mathcal{G}_{\mathcal{K}_{b,\parallel}}(\mathbf{r}_\parallel - \mathbf{r}'_\parallel, t) \left[\mathcal{G}_{\mathcal{K}_{b,\perp}}(z - z', t) - \mathcal{G}_{\mathcal{K}_{b,\perp}}(z + z', t)\right], \tag{22}$$

with the initial condition $\varphi(\mathbf{r}) = \delta(z - z')\delta(\mathbf{r}_\parallel)$. As can be seen, the agreement between the numerical simulation and the analytical results is very good, even though they are obtained by completely different models.

Figure 3 again shows a comparison between the analytical model and the numerical simulation, but this time by considering that, once particles are adsorbed, they can diffuse within the surface. In figure 3, the z-direction and the y-direction at the surface of the square displacement are shown. The numerical simulations are represented by the solid black line, while the analytical model corresponds to the red dashed line, and, as in the previous scenario, an agreement between the numerical and analytical model is verified. From both figures 2 and 3, a clear trend change of the diffusion over time is observed. As in figure 2, this change occurs both in the z- and y-directions, corresponding to the moment when particles reach the surface and start being adsorbed. The anomalous diffusion in the bulk is related to particles getting adsorbed by the surface at some rate, thus slowing down the process of particles reaching the surface in the bulk. Note that, in the initial moments, the usual diffusion is obtained because particles have not arrived at the surface yet. In figure 3, a behavior change is also observed, both in the bulk and at the surface. However, in the case with diffusion within the surface, the diffusive process remains normal (usual) in the bulk, even after particles reach the surface, displaying only a small transient behavior corresponding to the moment the first particles reach the wall. On the surface, on the other hand, from the moment particles start being adsorbed, the diffusive behavior quickly reaches an anomalous diffusion, i.e. characterized by a subdiffusion [42].

J. Stat. Mech. (2021) 113202

Now, with equations (15) and (20), and having set the validity of the model by comparing it to numerical simulations, we can analyze the behaviors of bulk and surface distributions. First, we look at the bulk distribution, which, as a 3D distribution, shows a spreading behavior, as shown in figure 4, for two different values of t' and by taking the initial condition $\rho(\mathbf{r},0)=\delta(\mathbf{r}_{\parallel})\delta(z-\bar{z})$ with $k_s(t)=\kappa\delta(t)$. Figure 5 shows the surface distribution at a fixed value of t' vs $r_{\parallel}$ for two different values of $k_d'=z'^2k_d/\mathcal{K}_{b,\parallel}$. The surface density follows a typical spreading behavior from the origin of $r_{\parallel}$ due to the surface diffusion.

As has been demonstrated in the literature [18, 36], depending on how diffusing particles interact with the surface, the diffusive process might be different from usual diffusion. This is often observed by keeping track of the MSD, which indicates if diffusion is standard or anomalous. In the first case, of standard diffusion, we have a linear time dependence, i.e. $\langle(r-\langle r\rangle)^2\rangle\sim t$, which is typical of Markovian processes. The second scenario implies in a nonlinear time dependence, e.g. $\langle(r-\langle r\rangle)^2\rangle\sim t^{\gamma}$, where $\gamma<1$ and $\gamma>1$ correspond to sub and superdiffusion, respectively. It is also possible to exist different behaviors such as $\langle(r-\langle r\rangle)^2\rangle\sim \ln^{\gamma}\,t$, which are related to an ultraslow diffusion [43]. Figure 6(a) shows the behavior of the MSD for the x-direction, i.e. $\sigma^2_{s,r_{\parallel}}(t)=\left\langle\left(r_{\parallel}-\langle r_{\parallel}\rangle\right)^2\right\rangle$, obtained from the distribution given by equation (15), which is connected to the particles diffusing on the surface. It is also interesting to note that for this scenario the diffusion is asymptotically characterized by the subdiffusive behavior with $\sigma_{s,r_{\parallel}}\sim t^{1/2}$. Similar behavior for the MSD was found in [44] by analyzing the diffusion in a backbone structure. In addition, the analysis of a random walk in a class of branched structures subjected to a mean drift induced by an external field in [45] shows an interplay between different two behaviors (anomalous and usual) of diffusion. Figure 6(b) shows the behavior of the MSD for the x-direction, i.e. $\sigma^2_{b,r_{\parallel}}(t)=\left\langle\left(r_{\parallel}-\langle r_{\parallel}\rangle\right)^2\right\rangle$, obtained from the distribution given by equation (20), which is connected to the particles diffusing in the bulk.

In figures 7(a) and (b), we show the behavior of $\sigma^2_{s,r_{\parallel}}(t)$ and $\sigma^2_{b,r_{\parallel}}(t)$ for two different time dependencies of $k_s(t)$, which implies different memory effects on the adsorption process. In particular, these choices for $k_s(t)$ imply the following asymptotic behaviors $\sigma^2_{b,r_{\parallel}}(t)\sim t$ (for $k_s(s)\propto 1/(1+\sqrt{s})$) and $\sigma^2_{b,r_{\parallel}}(t)\sim t+k\sqrt{t}$ (for $k_s(s)\propto 1/\sqrt{s}$) in the limit $t\to\infty$. The behavior of the MSD for the z-direction is shown in figure 8(a) and the reduced distribution $\rho_z(z,t)$, i.e. $\rho_z(z,t)=\int_{\mathcal{S}}\mathrm{d}\mathcal{A}'\,\rho(\mathbf{r},t)$, obtained from equation (20), is depicted in figure 8(b). From these figures, we may verify that the behavior of the particles on the surface, see figure 6(a), is anomalous with an initial transient, which is related to the choice of the initial condition. The particles in the bulk initially have a usual diffusion. For intermediate times, where the interaction with the surface is pronounced, the diffusion is anomalous, and for long times, the diffusion is usual.

J. Stat. Mech. (2021) 113202

4. Discussion and conclusions

We have investigated a diffusion process subjected to surface effects that may adsorb, desorb, and/or absorb (react). The particles on the surface may also diffuse, i.e. perform a lateral diffusion, before being desorbed from the surface to the bulk. The processes on the surface are coupled with the bulk equations through the boundary conditions, i.e. equation (3), which connects the flux of particles from the bulk to the surface with the density changes on the surface. Thus, the processes in the bulk modify the dynamics of the particles on the surface and vice-versa. We found the solutions for the diffusion of particles on the surface and for the particles in the bulk. In each case, we have also found the MSD and compared the analytical calculations and the numerical results obtained from the stochastic equations. In the bulk, the spreading may present an anomalous diffusion for an intermediate time, as shown in figures 6(b) and 7(b). For the spreading on the surface, we have an initial transient related to the initial condition, which considers the particles initially in the bulk. The diffusion on the surface initially presents a transient, which is followed by a subdiffusive behavior. Finally, we hope that the results present here are helpful to discuss diffusion processes that connect sorption and desorption (or reaction) mechanisms.

Acknowledgments

The authors are thankful to CNPq (Brazilian agency) for financial support. E K L also thanks the Lab-ATOMOS/UFRJ for the hospitality and support. R S Z thanks CNPq (304634/2020-4). Research developed with the support of LAMAP-UTFPR. P M N and F W T thank the National Agency for Petroleum, Natural Gas, and Biofuels (ANP) and Petrobras for financial support.

References

[1] Weiss M, Hashimoto H and Nilsson T 2007 Anomalous protein diffusion in living cells as seen by fluorescence correlation spectroscopy *Biophys. J.* **84** 4043–52
[2] Gal N and Weihs D 2010 Experimental evidence of strong anomalous diffusion in living cells *Phys. Rev.* E **81** 020903
[3] Evangelista L R and Lenzi E K 2018 *Fractional Diffusion Equations and Anomalous Diffusion* (Cambridge: Cambridge University Press)
[4] Lenzi E K, Zola R S, Ribeiro H V, Vieira D S, Ciuchi F, Mazzulla A, Scaramuzza N and Evangelista L R 2017 Ion motion in electrolytic cells: anomalous diffusion evidences *J. Phys. Chem* B **121** 2882–6
[5] Ribeiro de Almeida R R, Evangelista L R, Lenzi E K, Zola R S and Jákli A 2019 Electrical transport properties and fractional dynamics of twist-bend nematic liquid crystal phase *Commun. Nonlinear Sci. Numer. Simul.* **70** 248–56
[6] Gatenby R A and Gawlinski E T 1996 A reaction-diffusion model of cancer invasion *Cancer Res.* **56** 5745–53
[7] Cohen D S and Murray J D 1981 A generalized diffusion model for growth and dispersal in a population *J. Math. Biology* **12** 237–49
[8] Cantrell R S and Cosner C 1999 Diffusion models for population dynamics incorporating individual behavior at boundaries: applications to refuge design *Theor. Population Biol.* **55** 189–207
[9] Sonetaka N, Fan H-J, Kobayashi S, Chang H-N, Furuya E and Furuya E 2009 Simultaneous determination of intraparticle diffusivity and liquid film mass transfer coefficient from a single-component adsorption uptake curve *J. Hazard. Mater.* **164** 1447–51

J. Stat. Mech. (2021) 113202

[10] Bouzid M, Ben Torkia Y, Wjihi S and Ben Lamine A 2017 Kinetic adsorption modeling of ethanol molecules onto three types of activated carbons: microscopic interpretation of adsorption and diffusion parameters *J. Mol. Liq.* **242** 98–108
[11] Fontana K B, Lenzi G G, Watanabe E R L R, Lenzi E K, Pietrobelli J, Juliana A M T and Chaves E S 2016 Biosorption and diffusion modeling of Pb(II) by malt bagasse *Int. J. Chem. Eng.* **2016** 1–11
[12] Song J-J *et al* 2019 One-dimensional anomalous diffusion of gold nanoparticles in a polymer melt *Phys. Rev. Lett.* **122** 107802
[13] Wu J and Berland K M 2008 Propagators and time-dependent diffusion coefficients for anomalous diffusion *Biophys. J.* **95** 2049–52
[14] Alcázar-Cano N and Delgado-Buscalioni R 2018 A general phenomenological relation for the subdiffusive exponent of anomalous diffusion in disordered media *Soft Matter* **14** 9937–49
[15] Yurchenko I, Basso J M V, Syrotenko V S and Staii C 2019 Anomalous diffusion for neuronal growth on surfaces with controlled geometries *PLoS ONE* **14** e021618
[16] Zola R S, Lenzi E K, Evangelista L R and Barbero G 2007 Memory effect in the adsorption phenomena of neutral particles *Phys. Rev.* E **75** 042601
[17] Zola R S, Freire F C M, Lenzi E K, Evangelista L R and Barbero G 2007 Kinetic equation with memory effect for adsorption–desorption phenomena *Chem. Phys. Lett.* **438** 144–7
[18] Recanello M V, Lenzi E K, Martins A F, Li Q and Zola R S 2020 Extended adsorbing surface reach and memory effects on the diffusive behavior of particles in confined systems *Int. J. Heat Mass Transfer* **151** 119433
[19] Lomholt M A, van den Broek B, Kalisch S-M J, Wuite G J L and Metzler R 2009 Facilitated diffusion with DNA coiling *Proc. Natl Acad. Sci.* **106** 8204–8
[20] Oura K, Lifshits V G, Saranin A A, Zotov A V and Katayama M 2013 *Surface Science: An Introduction* (*Advanced Texts in Physics*) (Heidelberg: Springer)
[21] Ala-Nissila T, Ferrando R and Ying S C 2002 Collective and single particle diffusion on surfaces *Adv. Phys.* **51** 949–1078
[22] Eftekhari A 2019 Surface diffusion and adsorption in supercapacitors *ACS Sustain. Chem. Eng.* **7** 3692–701
[23] Ren W, Li G, Tian S, Sheng M and Geng L 2017 Adsorption and surface diffusion of supercritical methane in shale *Ind. Eng. Chem. Res.* **56** 3446–55
[24] Wu K, Li X, Guo C, Wang C and Chen Z 2016 A unified model for gas transfer in nanopores of shale-gas reservoirs: coupling pore diffusion and surface diffusion *SPE J.* **21** 1583–611
[25] Zhang Y and Fakhraai Z 2017 Decoupling of surface diffusion and relaxation dynamics of molecular glasses *Proc. Natl Acad. Sci. USA* **114** 4915–9
[26] Squires T M, Messinger R J and Manalis S R 2008 Making it stick: convection, reaction and diffusion in surface-based biosensors *Nat. Biotechnol.* **26** 417–26
[27] Penn A C, Zhang C L, Georges F, Royer L, Breillat C, Hosy E, Petersen J D, Humeau Y and Choquet D 2017 Hippocampal LTP and contextual learning require surface diffusion of AMPA receptors *Nature* **549** 384–8
[28] Pizzo M E *et al* 2018 Intrathecal antibody distribution in the rat brain: surface diffusion, perivascular transport and osmotic enhancement of delivery *J. Physiol.* **596** 445–75
[29] Chipot C and Comer J 2016 Subdiffusion in membrane permeation of small molecules *Sci. Rep.* **6** 35913
[30] Jeon J-H, Monne H M-S, Javanainen M and Metzler R 2012 *Phys. Rev. Lett.* **109** 188103
[31] Jeon J-H, Javanainen M, Seara H M, Metzler R and Vattulainen I 2016 *Phys. Rev.* X **6** 021006
[32] Roshandel R and Ahmadi F 2013 Effects of catalyst loading gradient in catalyst layers on performance of polymer electrolyte membrane fuel cells *Renew. Energy* **50** 921–31
[33] Gervais T and Jensen K F 2006 Mass transport and surface reactions in microfluidic systems *Chem. Eng. Sci.* **61** 1102–21
[34] Nazeeruddin M K, Baranoff E and Grätzel M 2011 Dye-sensitized solar cells: a brief overview *Sol. Energy* **85** 1172–8
[35] Lenzi E K, Lenzi M K, Zola R S, Ribeiro H V, Zola F C, Evangelista L R and Gonçalves G 2014 Reaction on a solid surface supplied by an anomalous mass transfer source *Physica* A **410** 399–406
[36] Guimarães V G, Ribeiro H V, Li Q, Evangelista L R, Lenzi E K and Zola R S 2015 Unusual diffusing regimes caused by different adsorbing surfaces *Soft Matter* **11** 1658–66
[37] Liu Y and Shen L 2008 From Langmuir kinetics to first- and second-order rate equations for adsorption *Langmuir* **24** 11625–30
[38] Scott Fogler H 2004 *Elements of Chemical Reaction Engineering* 3rd edn (Englewood Cliffs, NJ: Prentice-Hall)
[39] Crank J 1975 *The Mathematics of Diffusion* (Oxford: Oxford University Press)
[40] Arfken G B, Weber H J and Harris F E 2013 *Mathematical Methods for Physicists: A Comprehensive Guide* (Amsterdam: Elsevier)

J. Stat. Mech. (2021) 113202

[41] Kloeden P E and Platen E 1992 Stochastic differential equations *Numerical Solution of Stochastic Differential Equations* vols 103-60 (Heidelberg: Springer)
[42] Metzler R, Jeon J-H, Cherstvy A G and Barkai E 2014 *Phys. Chem. Chem. Phys.* **16** 24128–64
[43] Liang Y, Wang S, Chen W, Zhou Z and Magin R L 2019 A survey of models of ultraslow diffusion in heterogeneous materials *Appl. Mech. Rev.* **71** 040802
[44] Arkhincheev V E and Baskin E M 1991 Anomalous diffusion and drift in a comb model of percolation clusters *Sov. Phys. JETP* **73** 161–300
[45] Forte G, Burioni R, Cecconi F and Vulpiani A 2013 Anomalous diffusion and response in branched systems: a simple analysis *J. Phys.: Condens. Matter.* **25** 465106

J. Stat. Mech. (2021) 113202